Microarray Gridding by Mathematical Morphology

ROBERTO HIRATA JR.,
JUNIOR BARRERA,
RONALDO F. HASHIMOTO,
DANIEL O. DANTAS

Departamento de Ciência da Computação.
Instituto de Matemática e Estatística.
Universidade de São Paulo.
Rua do Matão 1010, 05508-900, São Paulo, SP, Brazil.
{hirata,jb,ronaldo,ddantas}@ime.usp.br

Abstract. DNA chips (i.e., microarrays) biotechnology is a hybridization (i.e., DNA matching) based process that makes possible to quantify the relative abundance of mRNA from two distinct samples by analysing their fluorescence signals. This technique requires robotic placement (i.e., spotting) of thousands of cDNAs (i.e., complementary DNA) in an array format on glass microscope slides which provide gene-specific hybridization targets. The two different samples of mRNA, usually labeled with Cy3 and Cy5 fluorochromes, are cohybridized onto each spotted gene and two digital images, one for each fluorochrome, are acquired after hybridization. Before estimating the signal and background of each spot, it is necessary to locate the region of the spot in order to map the gene information with the corresponding spot. Therefore, these images must be segmented for analysis, that is, the spotting geometric structure must be found. That implies segmenting the subarrays (i.e., the set of grouped spots) and, then, the positions of the spots in each subarray. In this paper, we introduce a new technique using morphological operators that performs automatic gridding procedures (i.e., subarrays and spots segmentation). This technique has been implemented and tested in a variety of microarray images with success.

1 Introduction

DNA chips (i.e., microarrays) biotechnology [6, 7] is a hybridization (i.e., DNA matching) based process that makes possible to quantitatively analyze fluorescence signals that represent the relative abundance of mRNA from two distinct samples. This technique requires robotic placement (i.e., spotting) of thousands of cDNAs (i.e., complementary DNAs) on glass microscope slides. This chip provides gene-specific hybridization targets. The samples of mRNA are labeled with different dyes (i.e., fluorochromes) and then cohybridized onto each spotted gene. The most used fluorochromes for tagging mRNA are Cy3 and Cy5.

The detection and quantization of the resulting hybridization is performed by a special scanner which measures the light emitted by fluorochrome molecules when excited by light at an appropriate wavelength. The location and intensities at each point are stored in an image structure. An example of a microarray image is shown in Fig. 1. This image shows one fourth of the Cy3 channel (or 6 subarrays of 12 by 32 spots each).

The dimensions of a typical microarray image is about 2000×6000 pixels, where each pixel represents a disk with $10\mu m$ of diameter.

The acquired DNA chip images have to be analyzed by Image Processing techniques in order to get the relative intensity of the Cy3 and Cy5 spot signals. The first step of this analysis is image segmentation (to generate a partition of the image pixels [3, 4]), that is, to segment the image subarrays and spots. The procedures that perform theses tasks are called, respectively, subarray and spot gridding. The subarray and spot segmentation are necessary to link gene database information with the measured spot signal. The spot segmentation is also useful for spot signal estimation.

All available commercial software we have tested use the region of interest (ROI) [3, 5] approach to locate spots. In these software, the user gives some parameters (number of subarray's rows and columns, number of spot's rows and columns for each subarray, distance from one spot to another, distance from one subarray to another, diameter of each spot and etc) and the software draws an array of ROIs, one for each spot. Usually the array of ROIs is far from good, obliging the user to go through a cumbersome step of adjusting the ROIs to the correct position.

In this paper, we introduce a new technique using morphological operators that performs automatic gridding procedures for subarray and spots. This technique has been implemented and tested with microarray images from several makers.

Following this introduction, Section 2 introduces the mathematical foundations necessary for presenting the new

1530-1834/01 $10.00 © 2001 IEEE

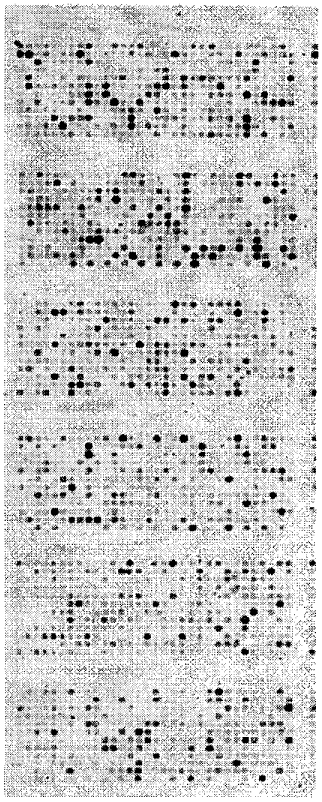

Figure 1: A microarray image.

technique. In Section 3, we present the proposed technique. In Section 4, we give some conclusions and future steps of this research.

2 Mathematical Foundations

In this section, we provide some definitions and properties necessary for understanding the morphological approach used for subarray and spots gridding in microarray images.

Let $\mathbf{Z}$ be the set of integers; the origin of $\mathbf{Z}^2$ is denoted $o = (0,0)$. Let E be a non-empty and finite subset of $\mathbf{Z}^2$ and let K be an interval $[0,k]$ of $\mathbf{Z}$, with $k > 0$. In this paper, we consider that E is an Abelian group with respect to a binary operation denoted by $+$.

A function f from E to K, $f \in K^E$, represents a *gray-scale image*. A *pixel*, or *point*, is an element of E, for instance, a $p \in E$ is a point in an image f and its gray-level is $f(p)$.

The *union* of two gray-scale images f_1 and f_2, denoted $f_1 \vee f_2$, is the function in K^E given by, for any $x \in E$, $(f_1 \vee f_2)(x) = \max\{f_1(x), f_2(x)\}$.

The *intersection* of two gray-scale images f_1 and f_2, denoted $f_1 \wedge f_2$, is the function in K^E given by, for any $x \in E$, $(f_1 \wedge f_2)(x) = \min\{f_1(x), f_2(x)\}$.

The *addition* of two gray-scale images f_1 and f_2, denoted $f_1 + f_2$, is the function in K^E given by, for any $x \in E$,

$$(f_1 + f_2)(x) = \begin{cases} f_1(x) + f_2(x) & \text{if } f_1(x) + f_2(x) \leq k \\ k & \text{otherwise} \end{cases}$$

The *reflection* of a subset $X \subseteq E$ is the subset $\check{X} = \{x \in E : -x \in X\}$.

For any $X \subseteq E$ and $y \in E$, X_y denotes the translation of X by y, that is, $X_y = \{x \in E : x - y \in X\}$.

The *dilation* and *erosion* ([1], p. 80) of a function f by a structuring element $B \subseteq E$ are, respectively, the functions $\delta_B(f)$ and $\varepsilon_B(f)$ in K^E given by, for any $x \in E$,

$$\delta_B(f)(x) = \max\{f(y) : y \in \check{B}_x \cap E\}$$

and

$$\varepsilon_B(f)(x) = \min\{f(y) : y \in B_x \cap E\}.$$

Given a structuring element $B \subseteq E$, the operators γ_B and ϕ_B from K^E to K^E, given by $\gamma_B = \delta_B\varepsilon_B$ and $\phi_B = \varepsilon_B\delta_B$ are called, respectively, *morphological opening* and *morphological closing* by B ([8], p. 50).

Let A and B be subsets of the 3×3 square. The operator $\nabla_{A,B}$ from K^E to K^E, given by $\nabla_{A,B} = \delta_A - \varepsilon_B$ is called *morphological gradient* ([8], p.437). This operator performs the enhancement of edges. Particularly, if A and B are two or three points line segments it does a directional enhancement of edges. If $B = \{o\}$, then the morphological gradient is called *external morphological gradient* and it is denoted ∇^e_A.

Let f be an element of K^E. The operators $\delta_{B,f}$ and $\varepsilon_{B,f}$ from K^E to K^E, given by $\delta_{B,f} = \delta_B \wedge f$ and $\varepsilon_{B,f} = \varepsilon_B \vee f$ are called *conditional dilation* and *conditional erosion* by B given f [8, p. 393].

Let n be a positive integer. The succession of n conditional dilations $\delta_{B,f}$ (respectively, erosions $\varepsilon_{B,f}$), denoted by $\delta^n_{B,f} = \delta_{B,f}\delta_{B,f}\cdots\delta_{B,f}$ (respectively, $\varepsilon^n_{B,f} = \varepsilon_{B,f}\,\varepsilon_{B,f}\cdots\varepsilon_{B,f}$) is called *n-conditional dilation* (respectively, *n-conditional erosion*).

Let g be an element of K^E. The operators $\gamma_{B,g}$ and $\phi_{B,g}$ from K^E to K^E, given by, for any $f \in K^E$, $\gamma_{B,g}(f) = \delta^\infty_{B,f}(g)$ and $\phi_{B,g}(f) = \varepsilon^\infty_{B,f}(g)$ are called *inf-reconstruction* and *sup-reconstruction* from the marker g [9].

Let h be a constant function in K^E and g be an element of K^E. The operator $\phi_{B,g+h}$ from K^E to K^E obtained by the sup-reconstruction from the marker $g + h$ is called *basin*.

Let $t \geq |E|$, let $i \longmapsto x_i$ be a numbering process of the elements of E (that is a bijection from $[1,\ldots,|E|] \subset \mathbf{N}$ to E) and let f be an element of K^E such that $f(x_i) = i$, for $x_i \in E$. The operator Λ_B from $\{0,t\}^E$ to K^E, given by,

for any $g \in \{0,t\}^E$, $\Lambda_B(g) = \gamma_{B,g\wedge f}(g)$ is called *labeling* of g [8, pg. 405]. Note that in $\Lambda_B(g)$ each point of a *connected component* [2] of g is associated to the same value. The labeling operator is fundamental for applications which depend on geometrical measures of the objects.

Given a point $(a,b) \in E$, we define $E_{x=a} \subseteq E$ as the line cutting E in the vertical direction at the coordinate (a,b), that is, $E_{x=a} = \{(a,y) \in E\}$. Similarly, we can define $E_{y=b} = \{(x,b) \in E\}$ as the line cutting E in the horizontal direction at the coordinate (a,b).

Given a gray-scale image $f : E \to K$, the *horizontal projection profile* of f, denoted by $P_h(f)$, is the function from $E_{x=0}$ to $\mathbf{Z}$, such that, for any $(0,k) \in E_{x=0}$,

$$P_h(f)(0,k) = \sum_{p \in E_{y=k}} f(p) \tag{1}$$

Analogously, we can define the *vertical projection profile* of f, denoted by $P_v(f)$, as the function from $E_{y=0}$ to $\mathbf{Z}$, such that, for any $(k,0) \in E_{y=0}$,

$$P_v(f)(k,0) = \sum_{p \in E_{x=k}} f(p) \tag{2}$$

A *regional maximum* (resp., *regional minimum*) $M \subset E$ of a function $f \in K^E$ is a connected component with a given value $f(p) = h$, $\forall p \in M$ (plateau at level h), such that every point in the neighborhood of M has a strictly lower (resp., higher) value. The regional maxima and the regional minima can be extracted from the functions by the morphological operators regional maximum, $\varrho_B^{\max}$, and regional minimum $\varrho_B^{\min}$ [10, 2].

3 Image Segmentation

In this section we show the main steps performed by the system to locate each spot in the microarray. Since the experiment gives us two images instead of one and assuming there is no registering problem (usually there is not because the images are acquired simultaneously), the system uses both images to extract the grid information. In our tests we used either union or addition of the two images and the results are equivalent. In the examples we give in this section, we used the union of the channels, i.e., $f = f_{Cy3} \vee f_{Cy5}$, where f_{Cy3} and f_{Cy5} are the Cy3 and Cy5 images, respectively.

We start by showing the correction of rotation, that is fundamental for the automatic segmentation technique presented in the next sections.

3.1 Correction of Rotation

The main group correction that may be necessary before the gridding step is the rotation. Figure 2 illustrates the distortion the software can correct so far. Of course there are other types of distortions that may occur, for instance, individual spot misalignment but we usually do not need to correct them.

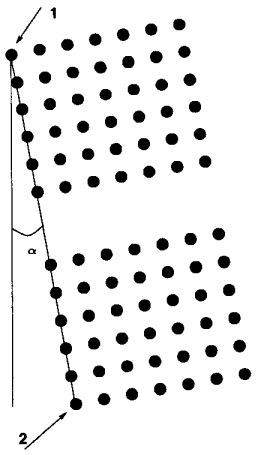

Figure 2: Rotation correction

The method for correction of rotation we propose here is human guided, works for small corrections (which is usually the case), and it is done via an interface where the user chooses 2 points to guide the program to compute the rotation angle. For instance, the center of the uppermost left spot and the center of the lowest left spot. Figure 2 also illustrates the process of choosing the two points, where the labelled arrows indicate the points and the order they have been chosen. The program computes the angle α and then corrects the rotation of a pixel $p = (x,y), \forall p \in E$, by translating it vertically by the nearest integer to $\tan(\alpha)(x - x_0)$, and horizontally by the nearest integer to $\tan(\alpha)(y - y_0)$, to the correct position, where (x_0, y_0) is the center of the image. It is important to notice that we can not use the usual rotation methods (linear, bilinear, bicubic, etc) because they change the value of the pixels. The part of the border that is lost by the rotation correction is not important because it does not contain hybridization information. An additional and optional step that is done before gridding is the extraction of the region (the central part) of the image that contains the spots, which is also human guided so far. Development is being done to automatize this part of the process that throws away the borders of the image.

3.2 Automatic Subarray Gridding

If the image is correctly aligned, the system can proceed to the next step, that is, to segment the regions of the subarrays. This is done by computing the projection profiles of the image f, filtering the profiles and computing the regional minima of each profile. The idea behind this pro-

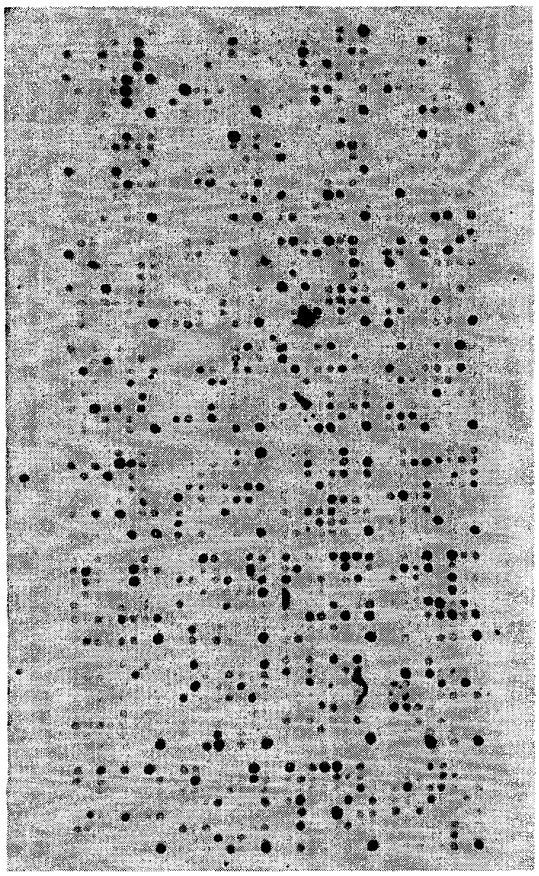

Figure 3: A more complex microarray image.

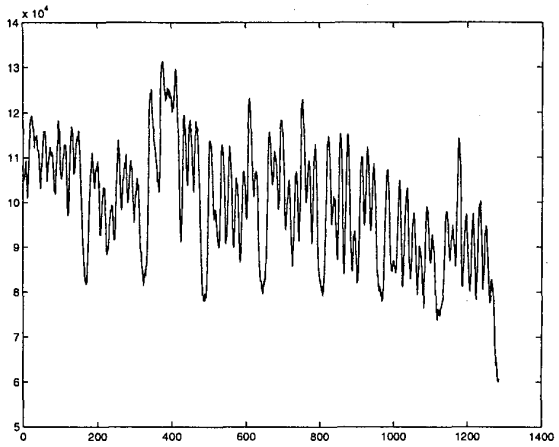

Figure 4: Horizontal microarray profile

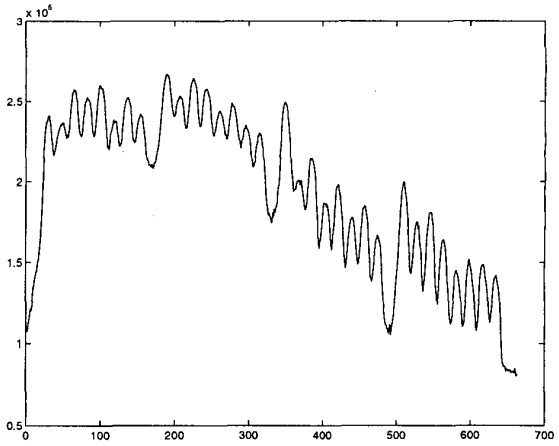

Figure 5: Vertical microarray profile

cedure is that the signal segmentation problem is easier. Therefore it is advantageous to transform an image segmentation to a signal segmentation problem. Once it is solved, we can take the solution back to the image realms. Figures 4 and 5 show the horizontal and vertical projection profiles of the image shown in Fig. 3 (an inversion has been done for a better visualization of the image).

Before proceeding the segmentation, a filtering step is necessary because noise or weak signal of a whole column, or a whole row, of subarrays can cause the misposition of one or more lines of the grid.

The first filter tries to remove all the noise due to the spot signals. The filter is a morphological closing, denoted by ϕ_{B_n}, where B_n is a flat $1 \times n$ structuring element. The parameter n is chosen based on the radius of the spot (it is approximately equal to the radius of the mean spot). This information is known because: the user adjusts the diameter of the spot during the spotting of the chip; and also adjusts the resolution of the scanner during digitalization. This in-

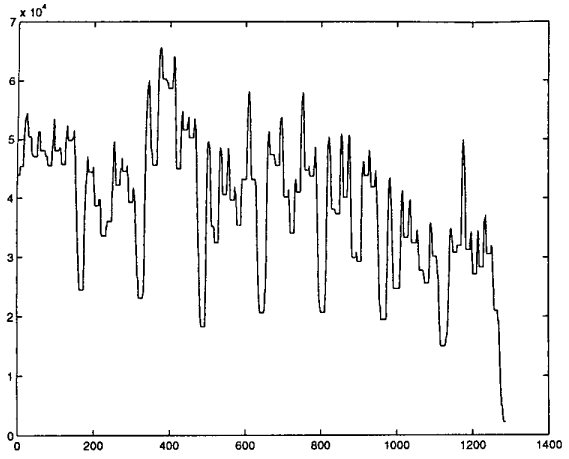

Figure 6: Result of the first filter

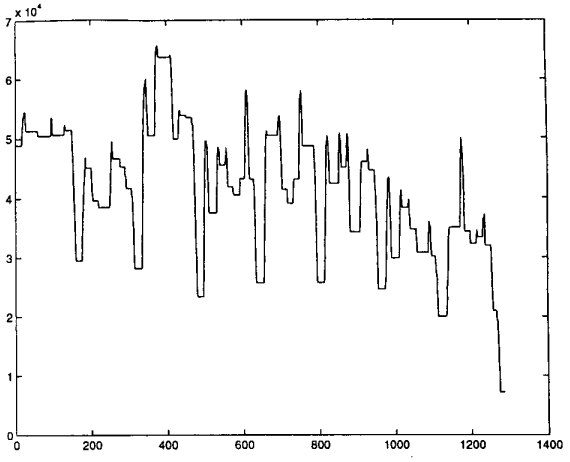

Figure 7: Result of the second filter

formation is usually stored in the header of the image file. The center of the structuring element B_n is at the left end. This is because operators are applied from left to right, the usual signal scan direction. Figure 6 illustrates the effect of this filter when applied to Fig. 4.

The second filter tries to remove all the valleys with medium contrast. This is necessary to eliminate noise inside the subarray region. The filtering is done by the operator *basin*, $\phi_{B_c,g+h}$, where h is the contrast threshold, g is the signal resulting from the first filter, and B_c is a 1×3 structuring element. Figure 7 illustrates the effect of the second filter when applied to Fig. 6.

The third filter is a morphological opening, γ_{B_m}, where B_m is a flat $1 \times m$ structuring element. The parameter m is given by the user based on the idea that the valleys between subarrays must be eliminated. Figure 8 illustrates the effect of the third filter when applied to Fig. 7.

The vertical and horizontal lines corresponding to the edges of the subarrays are the result of the union of the external morphological gradient of the regional minima applied to the result of the third filter for both profiles. There are 16 non zero pixels in the external morphological gradient signal whose coordinates correspond to the horizontal limits of the subarrays. Figure 9 shows the result of the subarray's segmentation (the image has been enlarged for a better visualization). The whole segmentation can be seen better in our web site http://www.vision.ime.usp.br/demos.html

Let B_c be a flat 1×3 structuring element. Let h, m and n be two non zero positive integers. Let $\varrho_B^{\min}$ be the regional minima operator and ∇_A^e be the external morphological gradient. The following equation summarizes the whole process for the horizontal profile $P_h(f)$. For the ver-

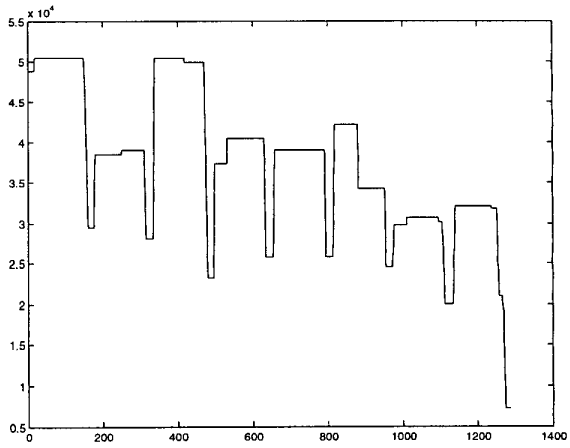

Figure 8: Result of the third filter

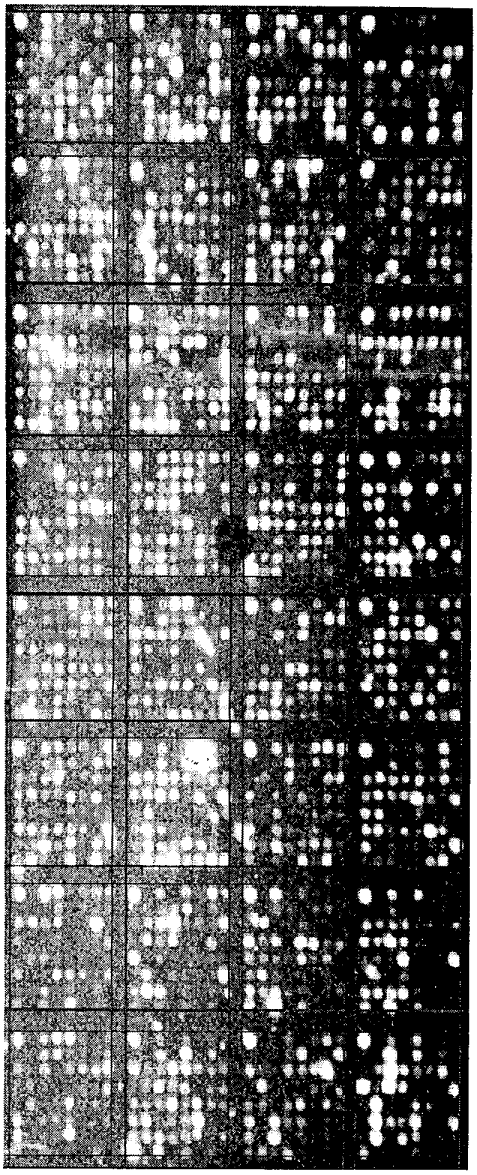

Figure 9: Result of the segmentation

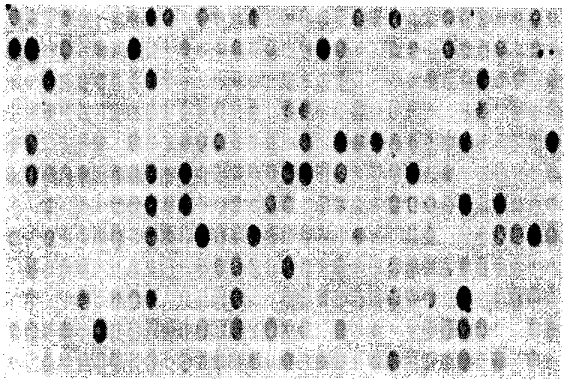

Figure 10: The union of two subarray image (Cy3 and Cy5).

tical profile the equation is similar.

$$\nabla_A^e(\varrho_{B_c}^{\min}(\gamma_{B_m}(\phi_{B_c,\phi_{B_n}(P_h(f))+h}(\phi_{B_n}(P_h(f)))))) \quad (3)$$

The coordinates of the non zero pixels of the horizontal and vertical filtered profiles can be used to extract the subarrays images. Usually those limits are tight, therefore the software allows the user to give a horizontal and a vertical looseness to be used in the extraction.

3.3 Automatic Spots Gridding

Each subarray is now extracted and the system can proceed to the next step, to segment the region of the spot. The idea is the same: the software computes the projection profiles of the subarray image, say f_i, where i is the index of the subarray, filters the profiles and takes the regional minima of each projection profile. The filter now is much simpler and the idea behind it is that only the spots (the places which we consider to be signal) will be responsible for the higher values in the profile, while the background points will be responsible for the lower values.

Figures 11 and 12 show the horizontal and vertical projection profiles of the image shown in Fig. 10.

Although being simpler, it is still necessary because noise or weak signals from a whole column, or row, of spots can cause the misposition of one or more lines of the grid. The filtering solution in this case is based on the fact that there is a regular grid imposed by the robot. The idea is to remove local minima between the minima that form the grid. This is done by a morphological opening with the same structuring element B_n used for subarray gridding. Figure 13 illustrates the filtering when applied to Fig. 11.

The whole process of horizontal gridding can be written by the following equation. The vertical gridding is equiv-

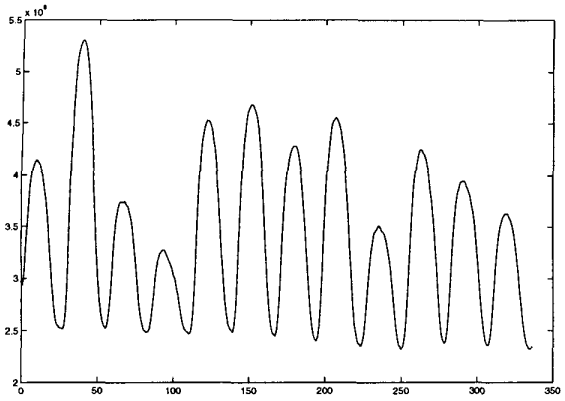

Figure 11: Horizontal subarray profile.

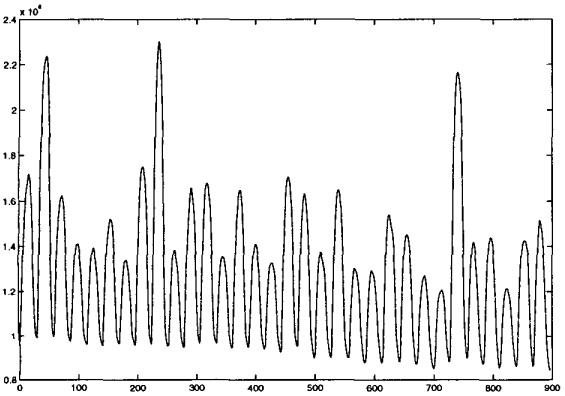

Figure 12: Vertical subarray profile.

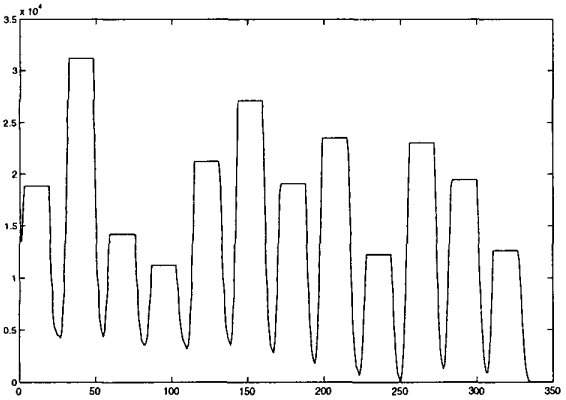

Figure 13: Subarray profile filtering.

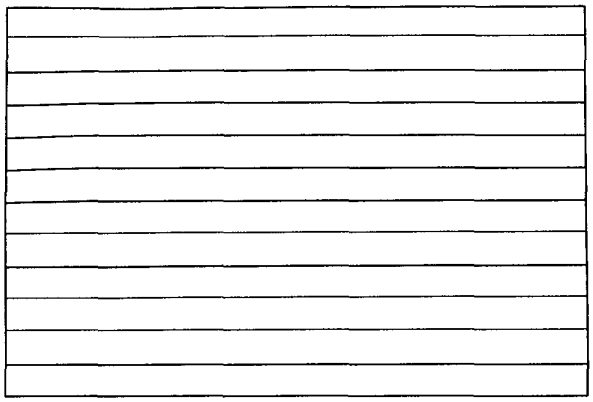

Figure 14: Vertical grid line.

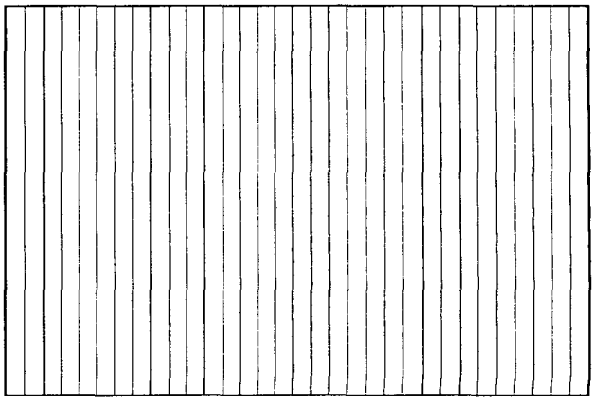

Figure 15: Horizontal grid lines

alent.

$$M_h = \varrho_{B_c}^{\min}(\gamma_{B_n}(P_h(f))) \tag{4}$$

The result of this segmentation, is a set of horizontal and vertical point coordinates (the non zero points of M_h and M_v, respectively) that define the horizontal and vertical lines of the grid. Figures 14 and 15 show the vertical and horizontal lines of the grid, respectively. Figure 16 shows the union of these images composed with the subarray image.

The complement of the grid is a set of squares, each containing a spot. Labeling this image using the morphological labeling operator produces another image where each point of each square has an integer value that can be used to map each spot to the corresponding entry in the gene database.

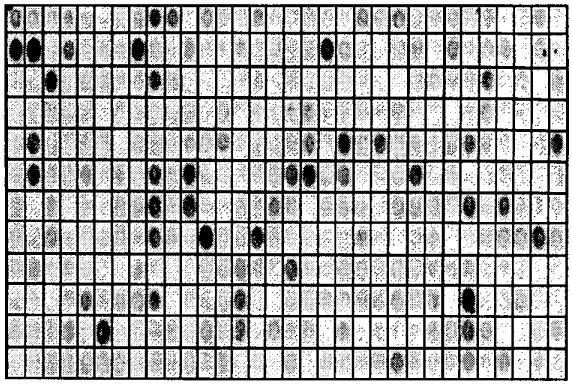

Figure 16: Resulting grid lines composed with subarray image

4 Conclusion

The gridding procedures to segment either the subarray's or the spot's regions in microarray images are usually done manually or with strong user assistance. This methodology is cumbersome, unreliable and non reproducible. Considering the regularity of the images, we have introduced a new gridding technique via morphological operators that is robust and automatic; user assistance is only necessary to fix image rotation and check if the segmentation is correct. The software has been implemented under Matlab using the MMach toolbox for mathematical morphology and tested with a variety of images from different microarray spotters and scanners. The result of the tests can be seen in our web site: http://www.vision.ime.usp.br/demos.html

The software provides an optional step to enforce a regularization of the griddings and adjust the intervals between each horizontal and vertical lines. This is valid if the subarray sizes are equal. This regularization can also be done with human assistance via a graphical interface that stops the processing if the number of subarrays are not the same as specified previously by the user. The segmentation of the spot's signals (from both images) is still an open problem that overwhelms the Image Processing fields. The source of difficulty is the fact that we have no access to the correct measure of the hybridization. Some controlled experiments are being done to find this answer.

5 Acknowledgment

The authors thank Prof. Hugo A. Armelin, Prof. E. Jordão Neves and Prof. Roberto M. César Jr. for having participate in the preliminary work of this research. The authors also thank Gustavo Henrique Esteves, Ricardo Z. N. Vêncio and Tie Koide who have contributed using the software and giving several suggestions for its improvement. The authors also thank Prof. Hamza El-Dorry, Prof. Gláucia M. Souza, Prof. Sandro J. Souza, Prof. Luiz F. L. Reis and Dr. Kátia Rocha for the microarray images used in the work.

References

[1] G. J. F. Banon and J. Barrera. Bases da Morfologia Matemática para Análise de Imagens Binárias. IX Escola de Computação, Pernambuco, Julho 1994.

[2] J. Barrera, G. J. F. Banon, R. A. Lotufo, and R. Hirata Jr. MMach: a Mathematical Morphology Toolbox for the Khoros System. *Electronic Imaging*, 7(1):174–210, 1998.

[3] R. C. Gonzalez and R. E. Woods. *Digital Image Processing*. Addison-Wesley Publishing Company, 1992.

[4] R. Hirata Jr. Segmentação de Imagens por Morfologia Matemática. Master's thesis, Instituto de Matemática e Estatística - USP, março 1997.

[5] Pratt. *Digital Image Processing*, chapter 18. Image Segmentation, pages 597–627. Wiley, 1991.

[6] M. Schena, R. A. Heller, T. P. Theriault, K. Konrad, E. Lachenmeier, and R. W. Davis. Microarrays: biotechnology's discovery platform for functional genomics. *Trends in Biotechnology*, 16(7):301–306, July 1998.

[7] M. Schena, D. Shalon, R. W. Davis, and P. O. Brown. Quantitative monitoring of gene expression patterns with a complementary DNA microarray. *Science*, 270:467–470, 1995.

[8] J. Serra. *Image Analysis and Mathematical Morphology*. Academic Press, London, 1982.

[9] J. Serra and L. Vincent. An overview of morphological filtering. *IEEE Transactions on Circuits, Systems and Signal Processing*, 11:47–108, 1992.

[10] L. Vincent. Morphological grayscale reconstruction in image analysis: efficient algorithms and applications. *IEEE Transactions on Image Processing*, 2:176–201, 1993.